

**A Comparison of the Reactivities of Dimethylsilylene (SiMe<sub>2</sub>) and Diphenylsilylene (SiPh<sub>2</sub>)  
in Solution by Laser Flash Photolysis Methods.**

Andrey G. Moiseev and William J. Leigh\*

<i>Photolysis of 9 in the presence of methoxytrimethylsilane (MeOTMS)</i>	S4
<b>Figure S1.</b> 600 MHz <sup>1</sup> H NMR spectrum of a 0.053 M solution of <b>9</b> in C <sub>6</sub> D <sub>12</sub> containing MeOTMS (0.19 M) and dioxane (0.02 M) after photolysis for 14 minutes with 254 nm light.	S5
<b>Figure S2.</b> Concentration vs. time plots for 254 nm irradiation of deoxygenated solutions of <b>9</b> (0.053 M) in C <sub>6</sub> D <sub>12</sub> containing MeOTMS (0.19 M) and dioxane (0.02 M).	S5
<i>Photolysis of 9 in the presence of acetic acid (AcOH)</i>	S6
<b>Figure S3.</b> 600 MHz <sup>1</sup> H NMR spectrum of a 0.039 M solution of <b>9</b> in C <sub>6</sub> D <sub>12</sub> containing AcOH (0.15 M) and dioxane (0.01 M) after photolysis for 14 minutes with 254 nm light.	S6
<b>Figure S4.</b> Concentration vs. time plots for 254 nm irradiation of deoxygenated solutions of <b>9</b> (0.039 M) in C <sub>6</sub> D <sub>12</sub> containing AcOH (0.15 M) and dioxane (0.01 M).	S7
<i>Photolysis of 9 in the presence of triethylgermane (Et<sub>3</sub>GeH)</i>	S7
<b>Figure S5.</b> 600 MHz <sup>1</sup> H NMR spectrum of a 0.045 M solution of <b>9</b> in C <sub>6</sub> D <sub>12</sub> containing Et <sub>3</sub> GeH (0.22 M) and dioxane (0.01 M) after photolysis for 14 minutes with 254 nm light.	S8
<b>Figure S6.</b> Concentration vs. time plots for 254 nm irradiation of deoxygenated solutions of <b>9</b> (0.045 M) in C <sub>6</sub> D <sub>12</sub> containing Et <sub>3</sub> GeH (0.2 M) and dioxane (0.01 M).	S8
<i>Photolysis of 9 in the presence of tri-<i>n</i>-butylstannane (Bu<sub>3</sub>SnH)</i>	S9
<b>Figure S7.</b> 600 MHz <sup>1</sup> H NMR spectrum of a 0.056 M solution of <b>9</b> in C <sub>6</sub> D <sub>12</sub> containing Bu <sub>3</sub> SnH (0.185 M) and dioxane (0.01 M) after photolysis for 14 minutes with 254 nm light.	S9
<b>Figure S8.</b> Concentration vs. time plots for 254 nm irradiation of deoxygenated solutions of <b>9</b> (0.056 M) in C <sub>6</sub> D <sub>12</sub> containing <i>n</i> -Bu <sub>3</sub> SnH (0.185 M) and dioxane (0.01 M).	S10
<i>Photolysis of 9 in the presence of 2,3-dimethyl-1,3-butadiene (DMB)</i>	S10
<b>Figure S9.</b> 600 MHz <sup>1</sup> H NMR spectrum of a 0.052 M solution of <b>9</b> in C <sub>6</sub> D <sub>12</sub> containing DMB (0.23 M) and dioxane (0.01 M) after photolysis for 14 minutes with 254 nm light.	S11
<b>Figure S10.</b> Concentration vs. time plots for 254 nm irradiation of deoxygenated solutions of <b>9</b> (0.05 M) in C <sub>6</sub> D <sub>12</sub> containing DMB (0.23 M) and dioxane (0.01 M).	S11
<i>Photolysis of 9 in the presence of bis(trimethylsilyl)acetylene (BTMSE)</i>	S12
<b>Figure S11.</b> Concentration vs. time plots for 254 nm irradiation of deoxygenated solutions of <b>9</b> (0.05 M) in C <sub>6</sub> D <sub>12</sub> containing bis(trimethylsilyl)acetylene (0.16 M) and dioxane (0.02 M).	S12

***Photolysis of 9 in the presence of CCl<sub>4</sub>***

S12

**Figure S12.** 600 MHz <sup>1</sup>H NMR spectrum of a 0.045 M solution of **9** in C<sub>6</sub>D<sub>12</sub> containing CCl<sub>4</sub> (0.20 M) and dioxane (0.01 M) after photolysis for 14 minutes with 254 nm light.

S13

**Figure S13.** Concentration vs. time plots for 254 nm irradiation of deoxygenated solutions of **9** (0.05 M) in C<sub>6</sub>D<sub>12</sub> containing CCl<sub>4</sub> (0.2 M) and dioxane (0.01 M).

S14

***Laser Flash Photolysis Experiments***

**Figure S14.** Plots of the pseudo-first order decay rate constants ( $k_{\text{decay}}$ ) for SiMe<sub>2</sub> (□) and SiPh<sub>2</sub> (○) vs. [THF] in hexane solution at 25 °C.

S14

**Figure S15.** (a) Plots of the pseudo-first order decay rate constants ( $k_{\text{decay}}$ ) for SiMe<sub>2</sub> (□) and SiPh<sub>2</sub> (○) vs. [MeOTMS] in hexane solution at 25 °C. (b) Transient absorption spectra recorded 64-90 ns (○) and 500-545 ns (□) after the laser pulse, for a  $5 \times 10^{-4}$  M solution of **1** in deoxygenated hexane containing 1.4 mM MeOTMS. The insets show decay traces recorded at 310 and 470 nm.

S15

**Figure S16.** Plots of the pseudo-first order decay rate constants ( $k_{\text{decay}}$ ) for SiMe<sub>2</sub> (□) and SiPh<sub>2</sub> (○) vs. [AcOH] in hexane solution at 25 °C.

S15

**Figure S17.** Plots of the pseudo-first order decay rate constants ( $k_{\text{decay}}$ ) for SiMe<sub>2</sub> (□) and SiPh<sub>2</sub> (○) vs. [O<sub>2</sub>] in hexane solution at 25 °C.

S16

**Figure S18.** Plots of the pseudo-first order decay rate constants ( $k_{\text{decay}}$ ) for SiMe<sub>2</sub> (□) and SiPh<sub>2</sub> (○) vs. [Et<sub>3</sub>SiH] in hexane solution at 25 °C.

S16

**Figure S19.** (a) Plots of the pseudo-first order decay rate constants ( $k_{\text{decay}}$ ) for SiMe<sub>2</sub> (□) and SiPh<sub>2</sub> (○) vs. [Bu<sub>3</sub>SnH] in hexane solution at 25 °C. (b) Transient absorption spectra recorded 32-96 ns (○) and 0.88-0.99 μs (□) after the laser pulse, for a 0.09 mM solution of **9** in deoxygenated hexane containing 1.0 mM Bu<sub>3</sub>SnH. The insets show decay traces recorded at 530 and 480 nm.

S17

**Figure S20.** Plots of the pseudo-first order decay rate constants ( $k_{\text{decay}}$ ) for SiMe<sub>2</sub> (□) and SiPh<sub>2</sub> (○) vs. [cyclohexene] in hexane solution at 25°C. (b) Transient absorption spectra recorded 48-112 ns (○), 0.64-0.70 μs (□), and 8.56-8.62 μs (Δ) after the laser pulse, for a 0.09 mM solution of **9** in deoxygenated hexane containing 0.6 mM cyclohexene. The insets show decay traces recorded at 280, 530, and 460 nm.

S18

**Figure S21.** Plot of the pseudo-first order decay rate constants ( $k_{\text{decay}}$ ) for SiMe<sub>2</sub> (□) and SiPh<sub>2</sub> (○) vs. [DMP] in hexane solution at 25 °C.

S18

**Figure S22.** (a) Plots of the pseudo-first order decay rate constants ( $k_{\text{decay}}$ ) for SiMe<sub>2</sub> (□) and SiPh<sub>2</sub> (○) vs. [DMB] in hexane solution at 25 °C. (b) Transient absorption spectra recorded 64-96 ns (○) and 0.62-0.74 μs (□) after the laser pulse, for a 0.09 mM solution of **9** in deoxygenated hexane containing 0.4 mM DMB. The insets show decay traces recorded at 280, 530 and 460 nm.

S19

**Figure S23.** Plots of the pseudo-first order decay rate constants ( $k_{\text{decay}}$ ) for SiMe<sub>2</sub> (□) and

S19

SiPh<sub>2</sub> (○) vs. [isoprene] in hexane solution at 25 °C.

**Figure S24.** (a) Plots of the pseudo-first order decay rate constants ( $k_{\text{decay}}$ ) for SiMe<sub>2</sub> (□) and SiPh<sub>2</sub> (○) vs. [BTMSE] in hexane solution at 25 °C. (b) Transient absorption spectra recorded 32-96 ns (○) and 0.88-0.99 μs (□) after the laser pulse, for a 0.09 mM solution of **9** in deoxygenated hexane containing 1.0 mM BTMSE. S20

**Figure S25.** (a) Plots of the pseudo-first order decay rate constants ( $k_{\text{decay}}$ ) for SiMe<sub>2</sub> (□) and SiPh<sub>2</sub> (○) vs. [TBE] in hexane solution at 25 °C. (b) Transient absorption spectra recorded 0-32 μs (○) and 1.01-1.12 ms (□) after the laser pulse, for a 0.09 mM solution of **9** in deoxygenated hexane containing 1.0 mM TBE. S21

**Figure S26.** Transient absorption spectra recorded 13-26 ns (○), 0.20-0.25 μs (□), and 1.48-1.53 μs (Δ) after the laser pulse, for a  $5 \times 10^{-4}$  M solution of **1** in deoxygenated hexane containing 0.6 mM CCl<sub>4</sub>. The insets show decay traces recorded at 460 and 360 nm. S22

**References**

S22

## Steady State Photolysis Experiments

### Photolysis of **9** in the presence of methoxytrimethylsilane (MeOTMS)

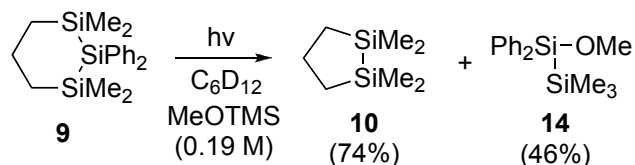
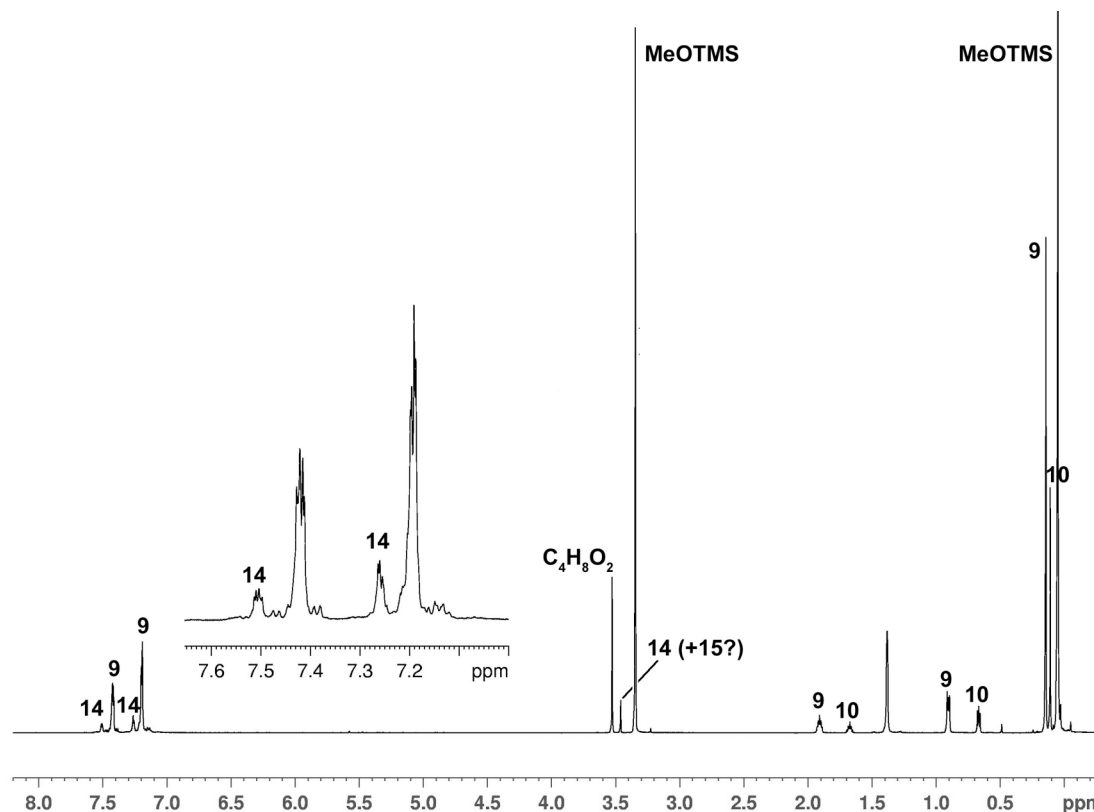
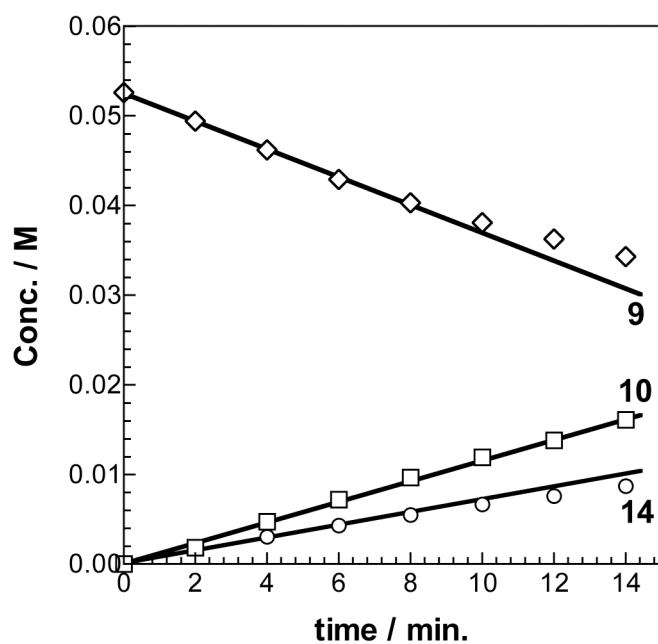


Figure S1 shows the NMR spectrum of the reaction mixture after 14 minutes photolysis (ca. 32% conversion of **9**). In addition to the characteristic resonances due to **10**, **9**, and MeOTMS, the spectrum shows a single methoxy resonance at  $\delta$  3.46 and new aromatic proton resonances centered at  $\delta$  7.50 and  $\delta$  7.26, which all grew in over the course of the photolysis. GC/MS analysis of the photolysate revealed there to be two products formed, of which the major eluted before **9** ( $m/z$  (I) = 286 (1,  $M^+$ ), 272 (28), 271 (100,  $M^+$ -Me), 255 (5, M-OMe), 213 (39, M-SiMe<sub>3</sub>), 211 (12), 209 (22), 194 (10), 193 (54), 183 (22), 105 (10), 73 (13), 59 (14), 45 (10)) and the minor eluted after **9** ( $m/z$  (I) = 468 (8,  $M^+$ ), 453 (40,  $M^+$ -Me), 395 (4,  $M^+$  - SiMe<sub>3</sub>), 375 (26), 365 (36), 364 (100), 303 (17), 298 (14), 287 (16), 260 (20), 213 (29), 183 (21), 105 (12)). The mass spectra are in reasonable agreement with the spectra reported for 1-methoxy-1,1-diphenyl-2,2,2-trimethyldisilane (**14**) and 1-methoxy-1,1,2,2-tetraphenyl-3,3,3-trimethyltrisilane (**15**), respectively.<sup>1</sup> The assignments were verified by <sup>1</sup>H NMR spectroscopy after removal of the solvent on the rotary evaporator and pumping on the resulting oil under vacuum (0.01 mm Hg) for 3 hours to remove **10** and excess methoxytrimethylsilane. The <sup>1</sup>H NMR spectrum of this mixture in benzene-*d*<sub>6</sub> showed it to consist of **9** (68 %) and two products (21% and 11%), exhibiting singlets at  $\delta$  3.457 and 3.433 in a 1:2 ratio, and at  $\delta$  0.219 and 0.215 in a 2:1 ratio, consistent with a 2:1 mixture of **14** and **15**.<sup>1</sup>

Concentration vs. time plots, constructed from the NMR integration data using the OMe proton resonances to quantitate **14**, are shown in Figure S2.



**Figure S1.** 600 MHz  $^1\text{H}$  NMR spectrum of a 0.053 M solution of **9** in  $\text{C}_6\text{D}_{12}$  containing MeOTMS (0.19 M) and dioxane (0.02 M) after photolysis for 14 minutes with 254 nm light.



**Figure S2.** Concentration vs. time plots for 254 nm irradiation of deoxygenated solutions of **9** (0.053 M) in  $\text{C}_6\text{D}_{12}$  containing MeOTMS (0.19 M) and dioxane (0.02 M; internal standard). The solid lines are the linear least squares fits of the data, and are characterized by the following slopes: **9**,  $-0.001555 \pm 0.000035$ ; **10**,  $0.001150 \pm 0.000019$ ; **14**,  $0.000712 \pm 0.000010$ .

*Photolysis of 9 in the presence of acetic acid (AcOH)*

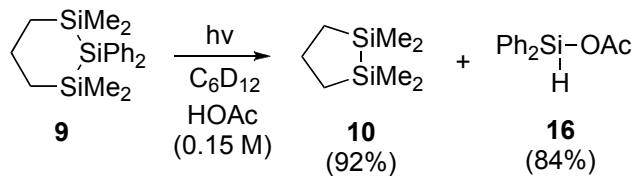
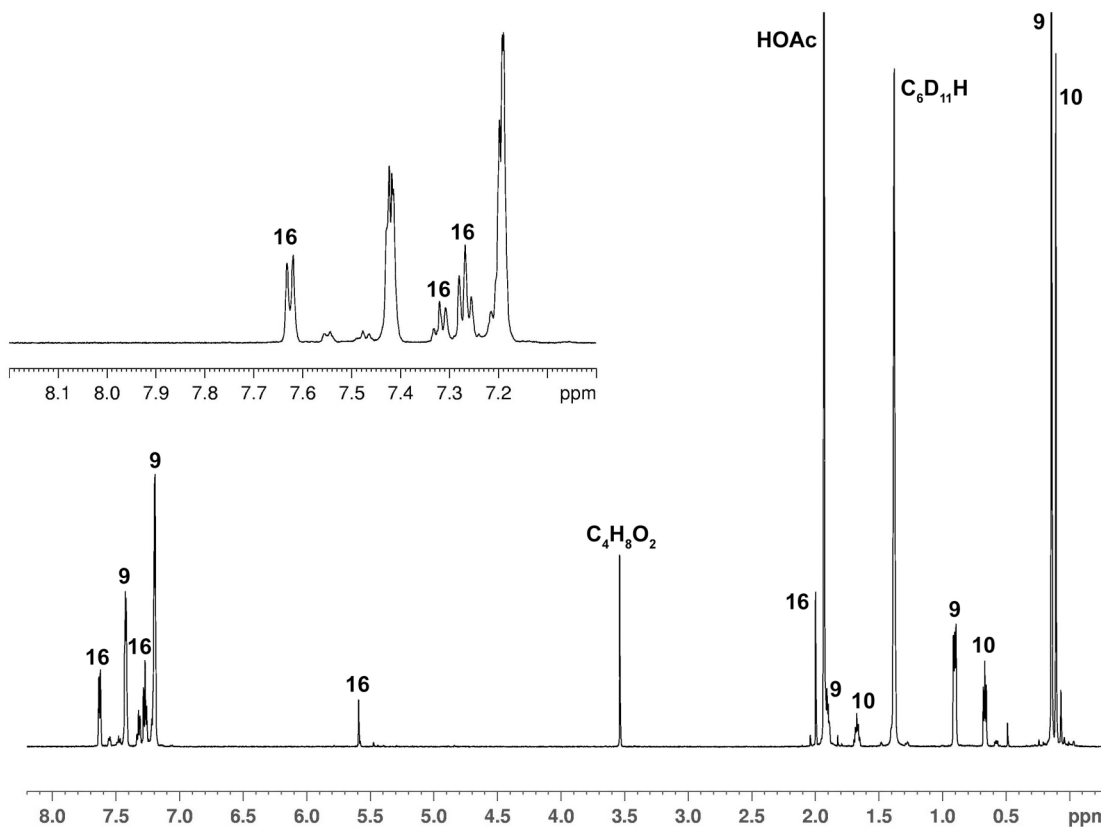
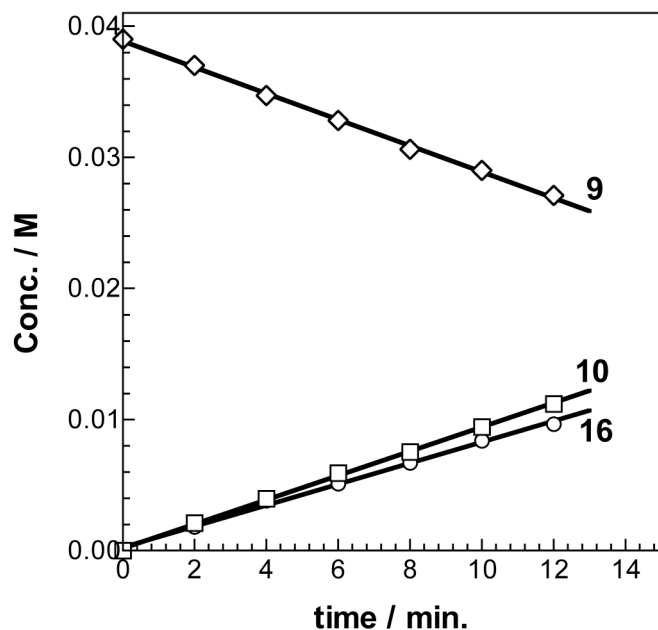


Figure S3 shows the NMR spectrum of the reaction mixture after 14 minutes photolysis (ca. 36% conversion of **9**). The two major products were identified as **10** and diphenylacetoxysilane (**16**;  $^1\text{H}$  NMR,  $\delta$  2.00 (s, 3H), 5.59 (s, 1H), 7.27 (t,  $J = 7.8$  Hz, 4H), 7.32 (t,  $J = 7.8$  Hz, 2H), 7.63 (d,  $J = 7.2$  Hz, 4H); GC/MS(EI),  $m/z$  (I) = 242 (7,  $\text{M}^+$ ), 241 (34), 207 (13), 199 (30), 181 (6), 165 (30), 164 (100), 136 (24), 123 (29), 122 (18), 78 (16), 77 (18), 51 (15), 50 (7), 45 (20), 44 (6), 43 (15)), the latter by comparison to the reported spectral data for this compound.<sup>2</sup> Concentration vs. time plots, constructed from the NMR integration data using the COMe proton resonance to quantitate **16**, are shown in Figure S4.



**Figure S3.** 600 MHz  $^1\text{H}$  NMR spectrum of a 0.039 M solution of **9** in  $\text{C}_6\text{D}_{12}$  containing AcOH (0.15 M) and dioxane (0.01 M) after photolysis for 14 minutes with 254 nm light.



**Figure S4.** Concentration vs. time plots for 254 nm irradiation of deoxygenated solutions of **9** (0.039 M) in  $C_6D_{12}$  containing AcOH (0.15 M) and dioxane (0.01 M). The solid lines are the linear least squares fits of the data, and are characterized by the following slopes: **9**,  $-0.000990 \pm 0.000015$ ; **10**,  $0.000915 \pm 0.000011$ ; **16**,  $0.000835 \pm 0.000035$ .

**Photolysis of 9 in the presence of triethylgermane ( $Et_3GeH$ )**

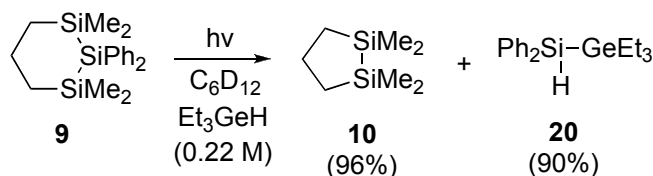
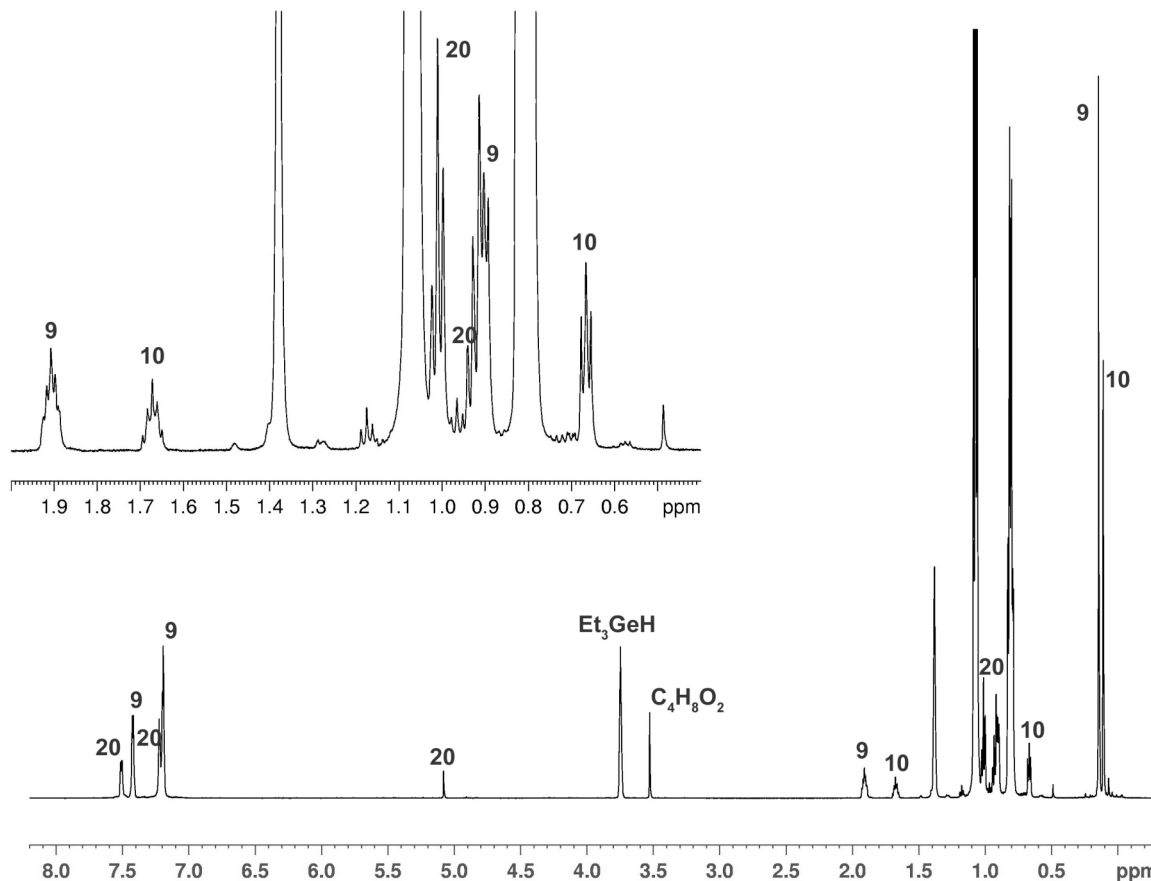
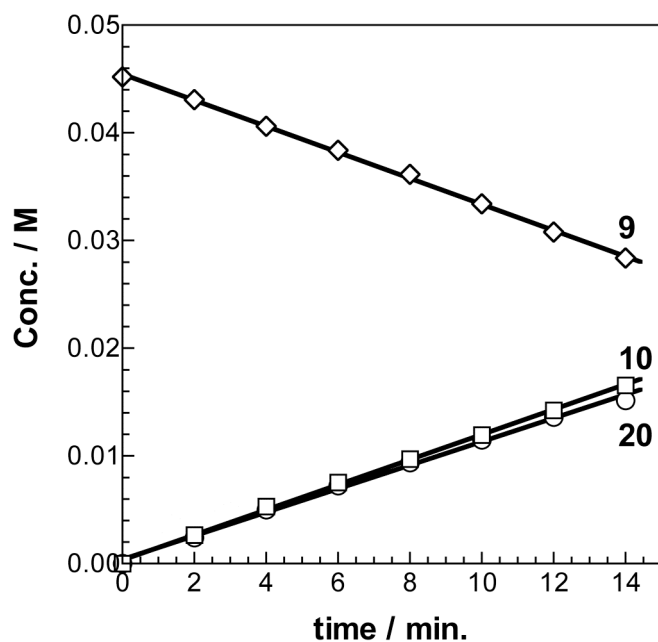


Figure S5 shows the NMR spectrum of the reaction mixture after 14 minutes photolysis (ca. 32% conversion of **9**). Triethyl(diphenylsilyl)germane (**20**; 90%) was identified as the major  $\text{SiPh}_2$ -derived product by comparison of its  $^1\text{H}$  and  $^{29}\text{Si}$  NMR and mass spectra to those of the authentic sample described above.

Concentration vs. time plots, constructed from the NMR integration data using the SiH proton resonance ( $\times 1.215$ , where the correction factor was determined from the NMR spectrum of the authentic sample) to quantitate **20**, are shown in Figure S6.



**Figure S5.** 600 MHz <sup>1</sup>H NMR spectrum of a 0.045 M solution of **9** in C<sub>6</sub>D<sub>12</sub> containing Et<sub>3</sub>GeH (0.22 M) and dioxane (0.01 M) after photolysis for 14 minutes with 254 nm light.



**Figure S6.** Concentration vs. time plots for 254 nm irradiation of deoxygenated solutions of **9** (0.045 M) in C<sub>6</sub>D<sub>12</sub> containing Et<sub>3</sub>GeH (0.22 M) and dioxane (0.01 M; internal standard). The solid lines are the linear least squares fits of the data, and are characterized by the following slopes: **9**,  $-0.001209 \pm 0.000017$ ; **10**,  $0.001166 \pm 0.000017$ ; **20**,  $0.001094 \pm 0.000026$ .

**Photolysis of **9** in the presence of tri-*n*-butylstannane (*Bu*<sub>3</sub>*SnH*)**

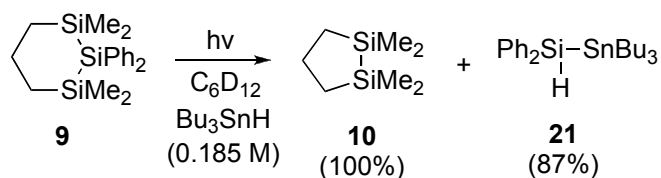
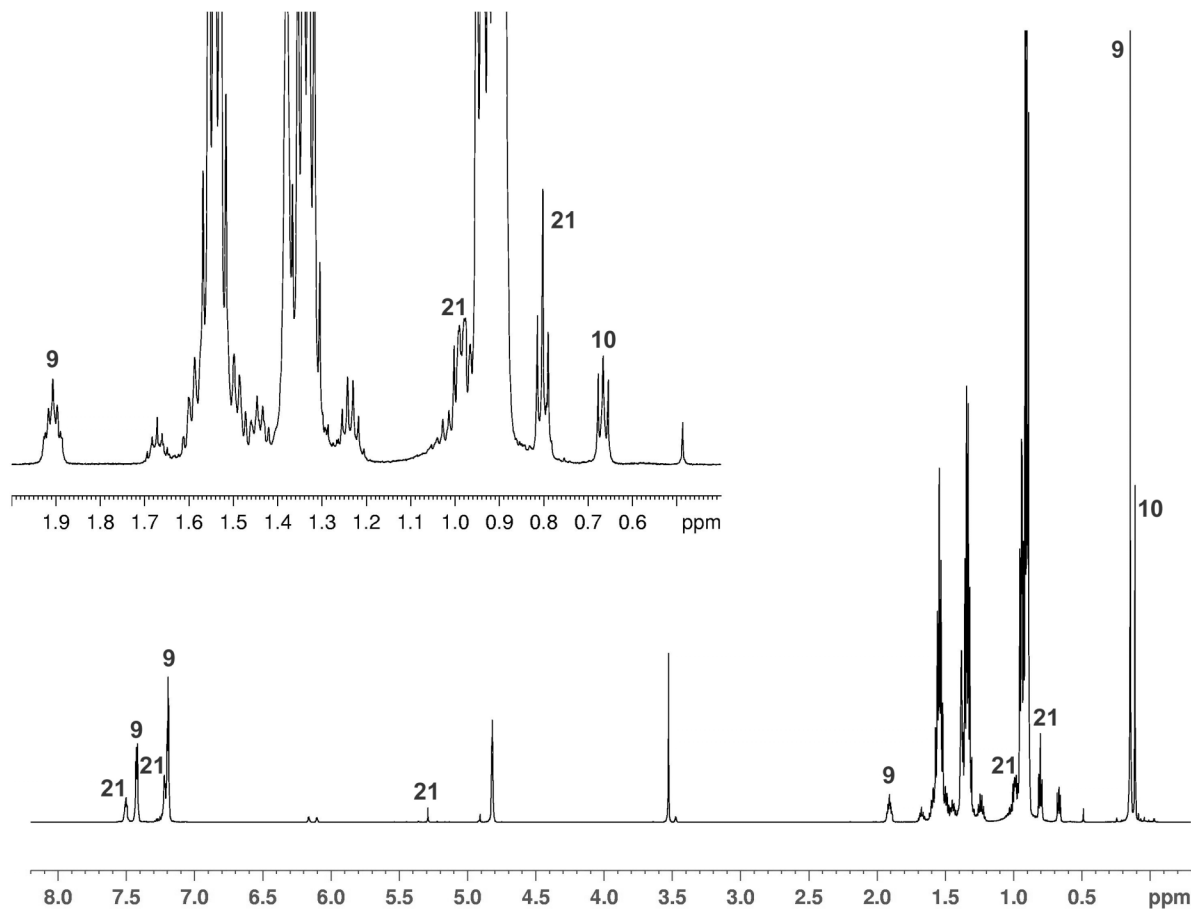
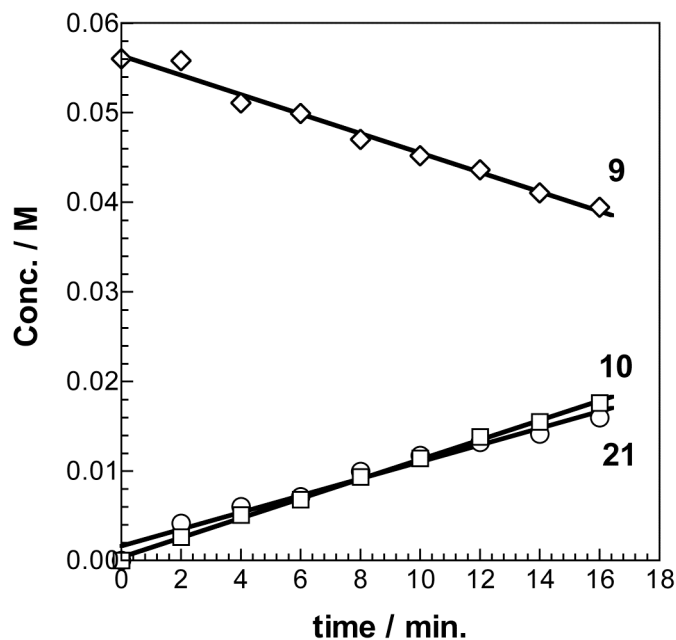


Figure S7 shows the NMR spectrum of the reaction mixture after 14 minutes photolysis (ca. 25% conversion of **9**). Tri-*n*-butyl(diphenylsilyl)stannane (**21**; 87%) was identified as the major SiPh<sub>2</sub>-derived product by comparison of its <sup>1</sup>H and <sup>29</sup>Si NMR and mass spectra to those of the authentic sample described above. Concentration vs. time plots, constructed from the NMR integration data using the CH<sub>3</sub> proton resonance to quantitate **21**, are shown in Figure S8.



**Figure S7.** 600 MHz <sup>1</sup>H NMR spectrum of a 0.056 M solution of **9** in C<sub>6</sub>D<sub>12</sub> containing Bu<sub>3</sub>SnH (0.185 M) and dioxane (0.01 M) after photolysis for 14 minutes with 254 nm light.



**Figure S8.** Concentration vs. time plots for 254 nm irradiation of deoxygenated solutions of **9** (0.056 M) in  $C_6D_{12}$  containing  $n\text{-Bu}_3\text{SnH}$  (0.185 M) and dioxane (0.01 M). The solid lines are the linear least squares fits of the data, and are characterized by the following slopes: **9**,  $-0.001085 \pm 0.000051$ ; **10**,  $0.001092 \pm 0.000018$ ; **21**,  $0.000940 \pm 0.000058$ .

**Photolysis of 9 in the presence of 2,3-dimethyl-1,3-butadiene (DMB)**

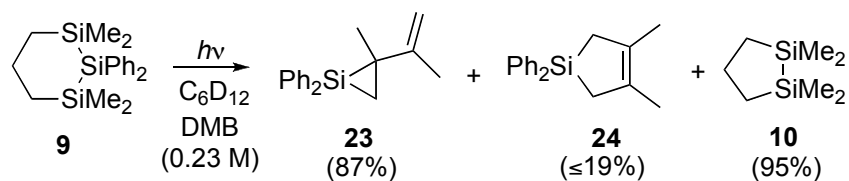
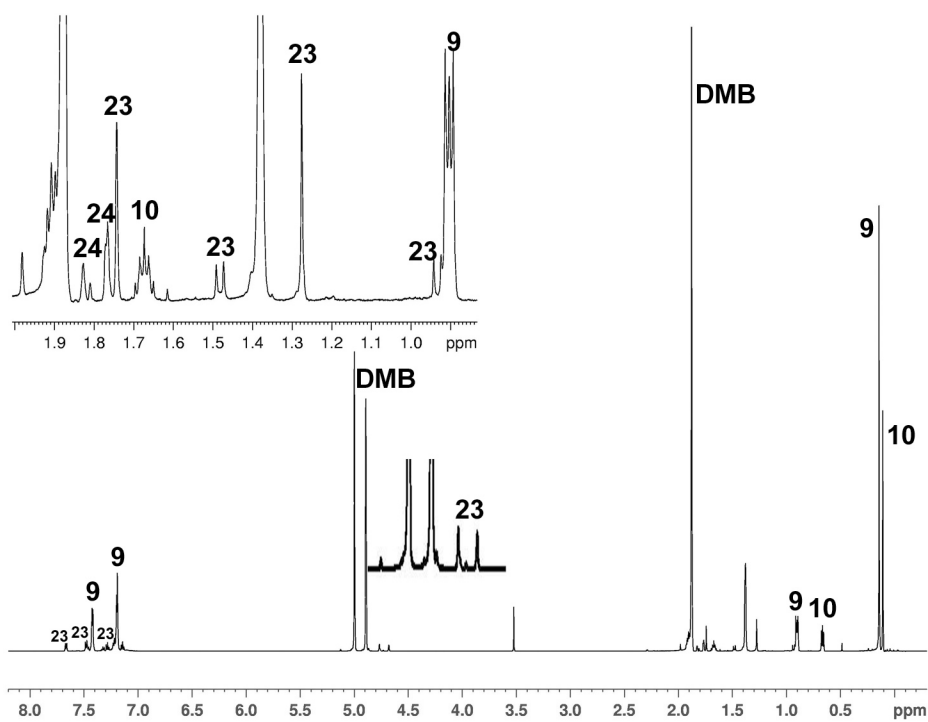
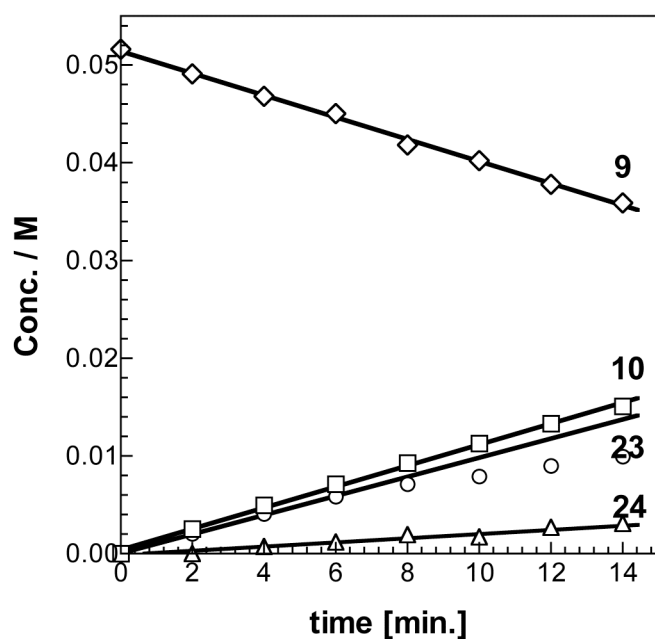


Figure S9 shows the NMR spectrum of the reaction mixture after 14 minutes photolysis (ca. 30% conversion of **9**). The three major products were identified as **10**, vinylsilirane **23**, and silacyclopent-3-ene **24**. **23** was identified on the basis of comparisons of its  $^1\text{H}$  and  $^{29}\text{Si}$  NMR spectra to that reported for the corresponding mesityl-substituted derivative:<sup>3</sup>  $^1\text{H}$  NMR,  $\delta$  0.93 (1H, d,  $J = 10.8$  Hz), 1.28 (3H, s), 1.48 (1H, d,  $J = 11.4$  Hz), 1.74 (3H, s), 4.68 (1H, s), 4.77 (1H, s), 7.14 (2H, t,  $J = 7.8$  Hz), 7.28 (2H, t,  $J = 7.8$  Hz), 7.33 (1H, t,  $J = 7.2$  Hz), 7.48 (3H, d,  $J = 7.8$  Hz), 7.66 (2H, dd,  $J = 7.2$  Hz, 1,2 Hz);  $^{29}\text{Si}$  NMR,  $\delta$  -63.72 (coupled to  $^1\text{H}$  resonances at  $\delta$  0.93, 1.28, and 1.48). Compound **24** was identified by comparison of its  $^1\text{H}$  and  $^{29}\text{Si}$  NMR and mass spectrum to that of an authentic sample.<sup>4</sup> GC/MS analysis of the product mixture showed peaks due only to **9**, **10**, and **23**. Concentration vs. time plots are shown in Figure S10.

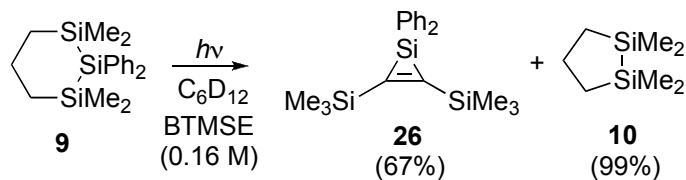


**Figure S9.** 600 MHz  $^1\text{H}$  NMR spectrum of a 0.05 M solution of **9** in  $\text{C}_6\text{D}_{12}$  containing DMB (0.23 M) and dioxane (0.01 M) after photolysis for 14 minutes with 254 nm light.



**Figure S10.** Concentration vs. time plots for 254 nm irradiation of deoxygenated solutions of **9** (0.05 M) in  $\text{C}_6\text{D}_{12}$  containing DMB (0.23 M) and dioxane (0.01 M). The solid lines are the linear least squares fits of the data, and are characterized by the following slopes: **9**,  $-0.001127 \pm 0.000025$ ; **10**,  $0.001076 \pm 0.000023$ ; **23**,  $0.000979 \pm 0.000025$ ; **24**,  $0.000214 \pm 0.000033$ .

**Photolysis of **9** in the presence of bis(trimethylsilyl)acetylene (BTMSE)**



Photolysis of a 0.05 M solution of **9** in  $\text{C}_6\text{D}_{12}$  containing bis(trimethylsilyl)acetylene (0.16 M) and dioxane (0.02 M) led to the formation of **10** and one major  $\text{SiPh}_2$ -containing product, which was identified as 1,1-diphenyl-2,3-bis(trimethylsilyl)silirene (**26**) on the basis of the following spectroscopic data of the crude reaction mixture after 24 minutes photolysis (ca. 53% conversion of **9**):  $^1\text{H}$  NMR,  $\delta$  0.22 (s, 18H), 7.15-7.25 (m, 6H), 7.45 (dd,  $J = 1.8, 8.4$  Hz, 4H);  $^{29}\text{Si}$  NMR,  $\delta$  -11.37 ( $\text{SiMe}_3$ ), -114.46 ( $\text{SiPh}_2$ ). Concentration vs. time plots, constructed from the NMR integration data using the  $\text{SiMe}_3$  proton resonance to quantitate **26**, are shown in Figure S11.

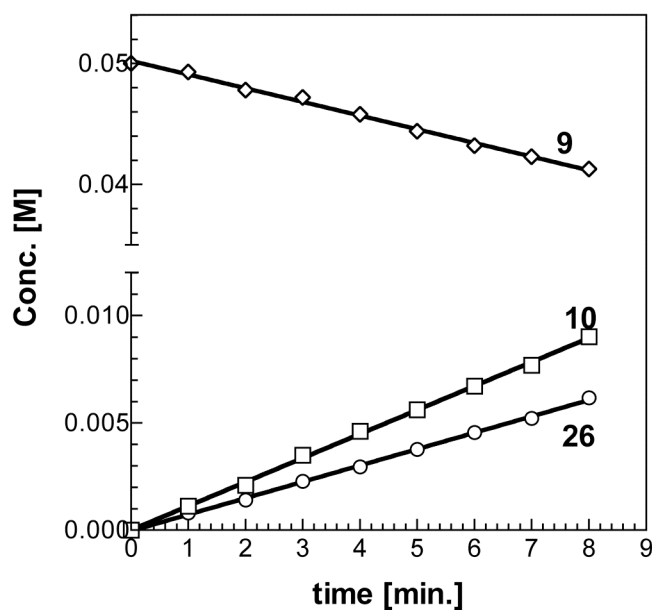


**Figure S11.** Concentration vs. time plots for 254 nm irradiation of deoxygenated solutions of **9** (0.05 M) in  $\text{C}_6\text{D}_{12}$  containing bis(trimethylsilyl)acetylene (0.16 M) and dioxane (0.02 M). The solid lines are the linear least squares fits of the data, and are characterized by the following slopes: **9**,  $-0.001131 \pm 0.000029$ ; **10**,  $0.001119 \pm 0.000014$ ; **26**,  $0.000762 \pm 0.000010$ .

**Photolysis of **9** in the presence of  $\text{CCl}_4$**

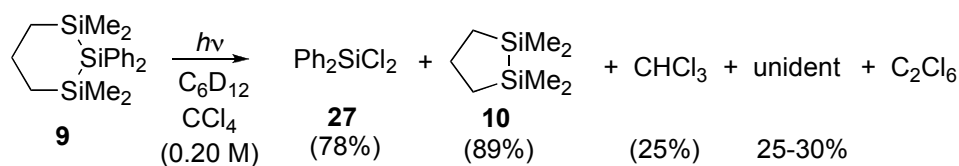
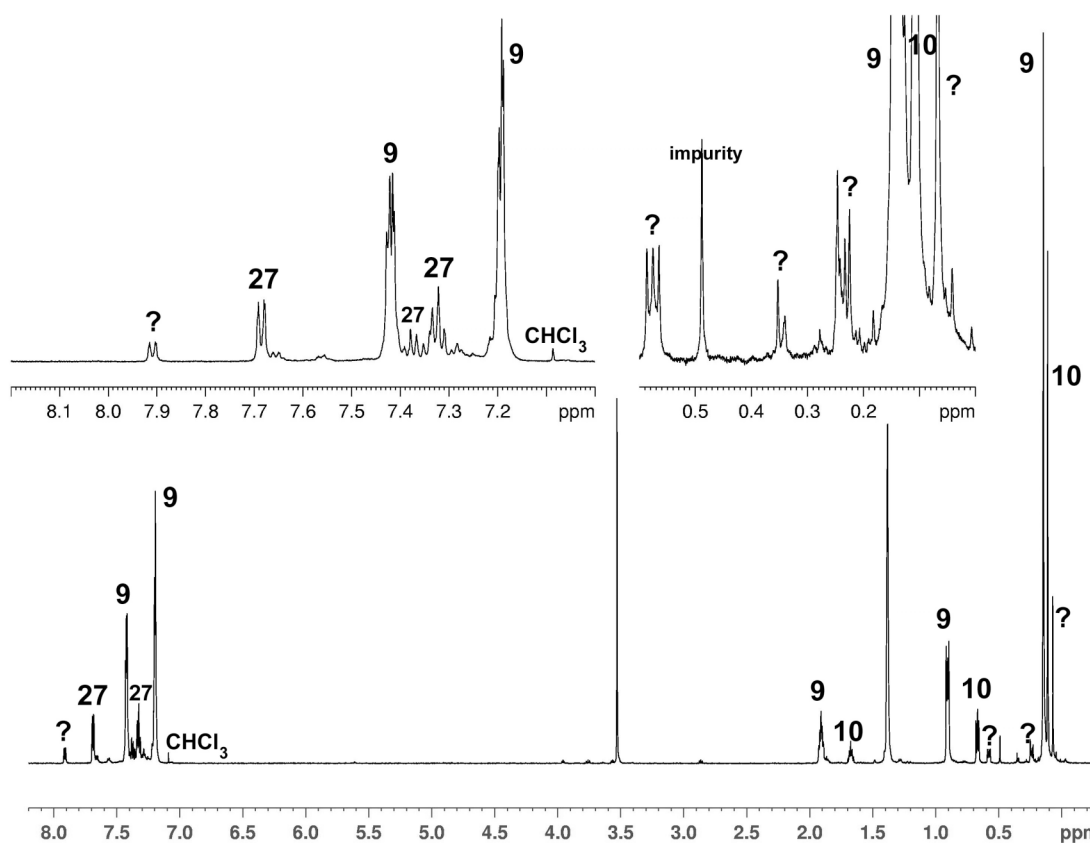
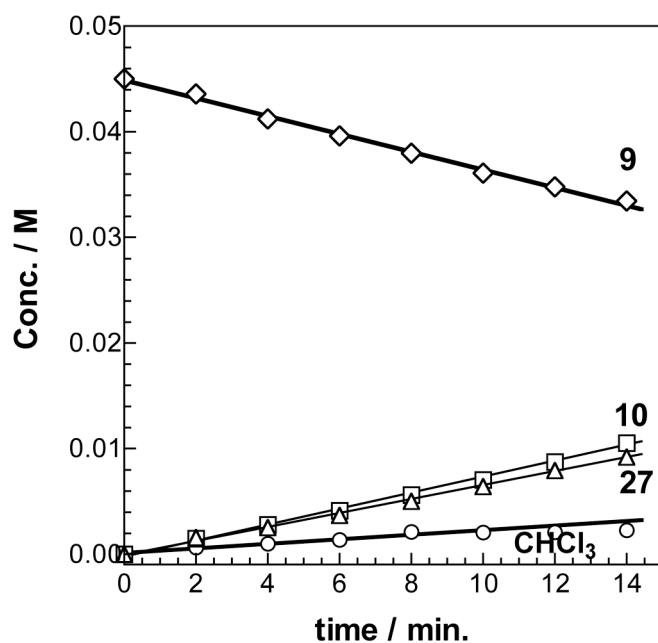


Figure S12 shows the NMR spectrum of the reaction mixture after 14 minutes photolysis (ca. 30% conversion of **9**). The three major products were identified as **10**, dichlorodiphenylsilane (**27**), chloroform and a minor unidentified product exhibiting (*inter alia*) a doublet at  $\delta$  7.94. Compound **27** and  $\text{CHCl}_3$  were identified by spiking the crude photolysates with small amounts of authentic samples, with secondary confirmation by GC/MS in the case of **27**. Hexachloroethane ( $\text{C}_2\text{Cl}_6$ ) was similarly identified by GC/MS spiking experiments. Concentration vs. time plots, constructed from the NMR integration data using the 4H doublet ( $\delta$  7.69) to quantitate **27**, the signals at  $\delta$  7.91 and  $\delta$  0.57 (4H assumed for each) to quantitate the unknown product(s), the average of the 2H and 4H multiplets to quantitate **10**, and the 2H multiplet to quantitate **9**, are shown in Figure S13. The normalized area of the 4H multiplet due to **9** ( $\delta$  0.89) decreased  $\sim$ 20% more slowly than that of the 2H multiplet ( $\delta$  1.9) with photolysis time, suggesting it contains an underlying product signal.



**Figure S12.** 600 MHz  $^1\text{H}$  NMR spectrum of a 0.045 M solution of **9** in  $\text{C}_6\text{D}_{12}$  containing  $\text{CCl}_4$  (0.20 M) and dioxane (0.01 M) after photolysis for 14 minutes with 254 nm light.



**Figure S13.** Concentration vs. time plots for 254 nm irradiation of deoxygenated solutions of **9** (0.045 M) in  $C_6D_{12}$  containing  $CCl_4$  (0.20 M) and dioxane (0.01 M). The solid lines are the linear least squares fits of the data, and are characterized by the following slopes: **9**,  $-0.000849 \pm 0.000019$ ; **10**,  $0.000758 \pm 0.000017$ ; **27**,  $0.000662 \pm 0.000013$ ;  $CHCl_3$ ,  $0.000217 \pm 0.000023$ ; unidentified (not shown),  $0.000211 \pm 0.000003$  and  $0.000256 \pm 0.000007$ .

## Laser Flash Photolysis Experiments

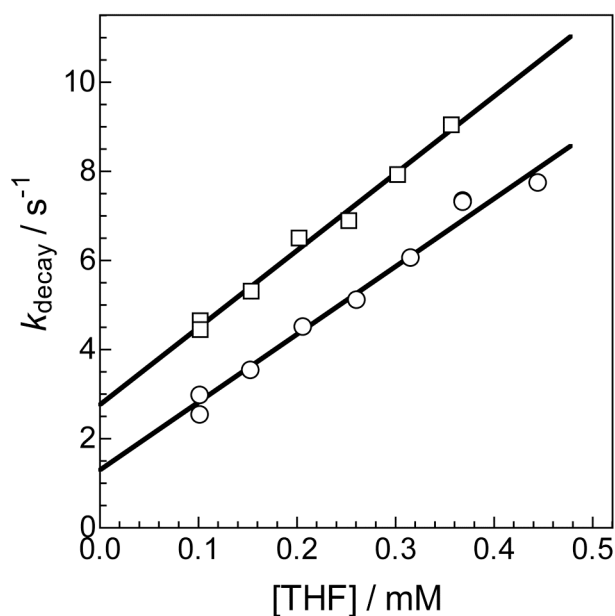


**Figure S14.** Plots of the pseudo-first order decay rate constants ( $k_{decay}$ ) for  $SiMe_2$  ( $\square$ ) and  $SiPh_2$  ( $\circ$ ) vs. [THF] in hexane solution at 25 °C. The solid lines are the linear least squares fits of the data to equation 6 in the paper.

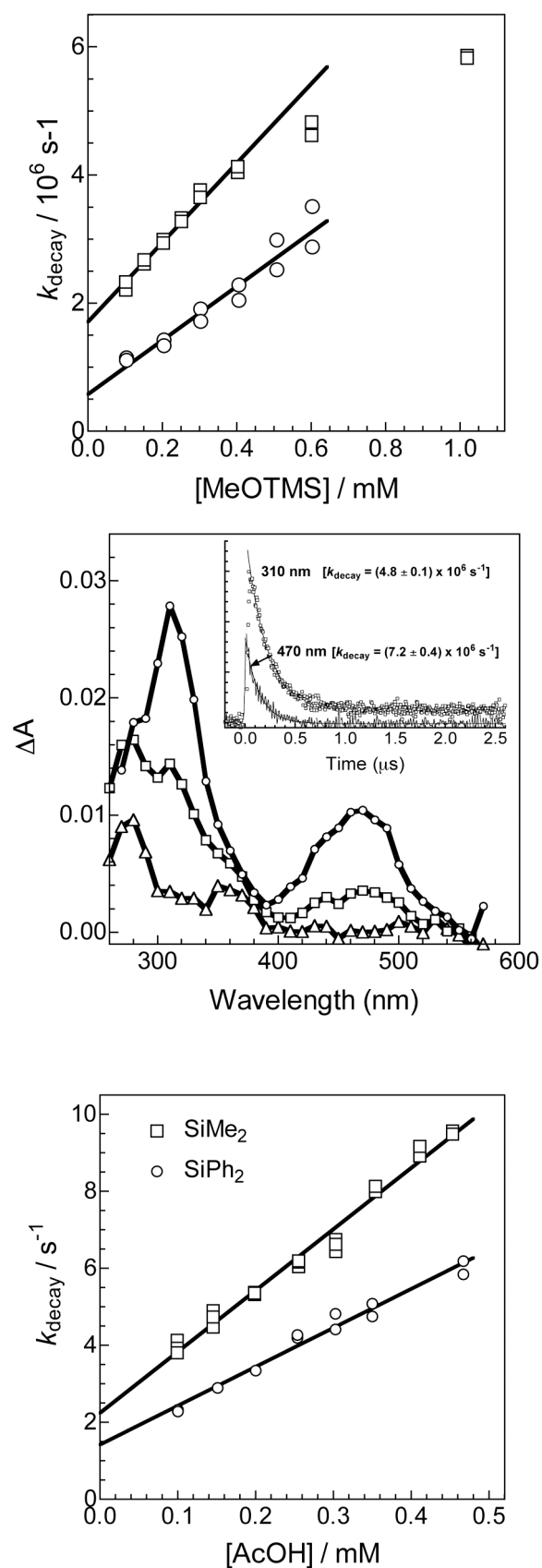


**Figure S15.** (a) Plots of the pseudo-first order decay rate constants ( $k_{\text{decay}}$ ) for SiMe<sub>2</sub> (□) and SiPh<sub>2</sub> (○) vs. [MeOTMS] in hexane solution at 25 °C. The solid lines are the linear least squares fits of the data to equation 6 in the paper.

**Figure S15.** (b) Transient absorption spectra recorded 70-96 ns (○), 230-275 ns (□), and 870-915 ns (Δ) after the laser pulse, for a  $5 \times 10^{-4}$  M solution of **1** in deoxygenated hexane containing 1.4 mM MeOTMS. The insets show decay traces recorded at 310 and 470 nm.

**Figure S16.** Plots of the pseudo-first order decay rate constants ( $k_{\text{decay}}$ ) for SiMe<sub>2</sub> (□) and SiPh<sub>2</sub> (○) vs. [AcOH] in hexane solution at 25 °C. The solid lines are the linear least squares fits of the data to equation 6 in the paper.

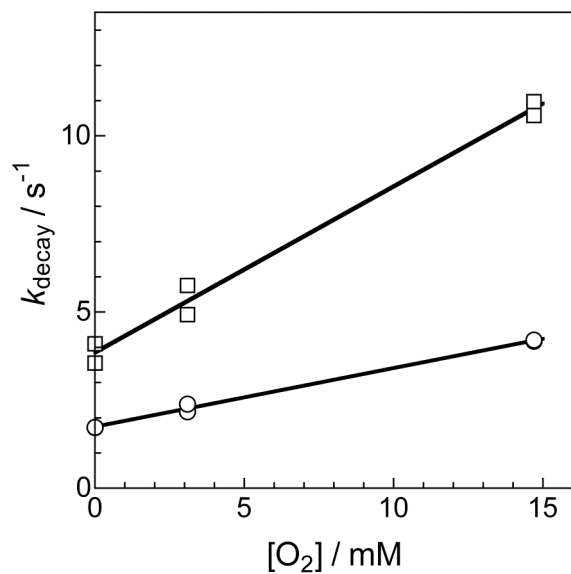


**Figure S17.** Plots of the pseudo-first order decay rate constants ( $k_{\text{decay}}$ ) for  $\text{SiMe}_2$  ( $\square$ ) and  $\text{SiPh}_2$  ( $\circ$ ) vs.  $[\text{O}_2]$  in hexane solution at 25 °C. The solid lines are the linear least squares fits of the data to equation 6 in the paper.

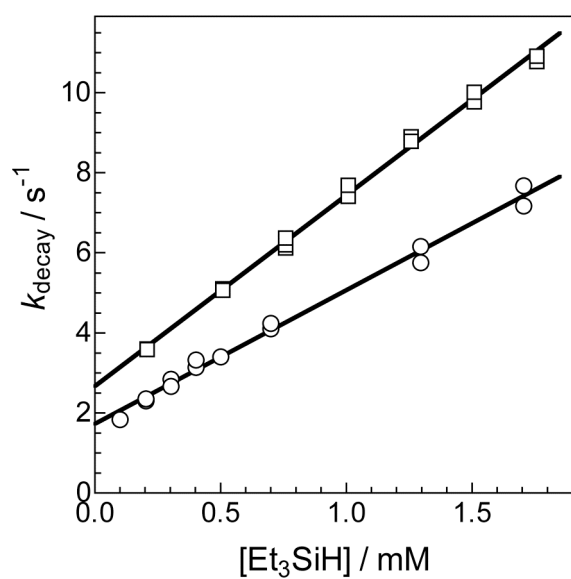


**Figure S18.** Plots of the pseudo-first order decay rate constants ( $k_{\text{decay}}$ ) for  $\text{SiMe}_2$  ( $\square$ ) and  $\text{SiPh}_2$  ( $\circ$ ) vs.  $[\text{Et}_3\text{SiH}]$  in hexane solution at 25 °C. The solid lines are the linear least squares fits of the data to equation 6 in the paper.

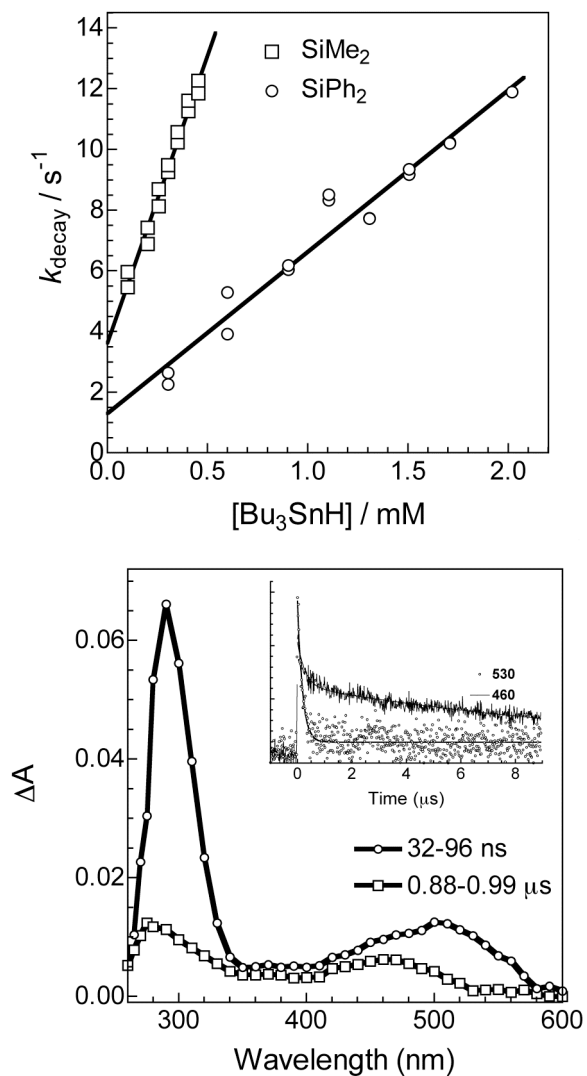


**Figure S19.** (a) Plots of the pseudo-first order decay rate constants ( $k_{\text{decay}}$ ) for  $\text{SiMe}_2$  ( $\square$ ) and  $\text{SiPh}_2$  ( $\circ$ ) vs.  $[\text{Bu}_3\text{SnH}]$  in hexane solution at 25 °C. The solid lines are the linear least squares fits of the data to equation 6 in the paper.

**Figure S19.** (b) Transient absorption spectra recorded 32-96 ns ( $\circ$ ) and 0.88-0.99  $\mu\text{s}$  ( $\square$ ) after the laser pulse, for a 0.09 mM solution of **9** in deoxygenated hexane containing 1.0 mM  $\text{Bu}_3\text{SnH}$ . The insets show decay traces recorded at 530 and 480 nm.

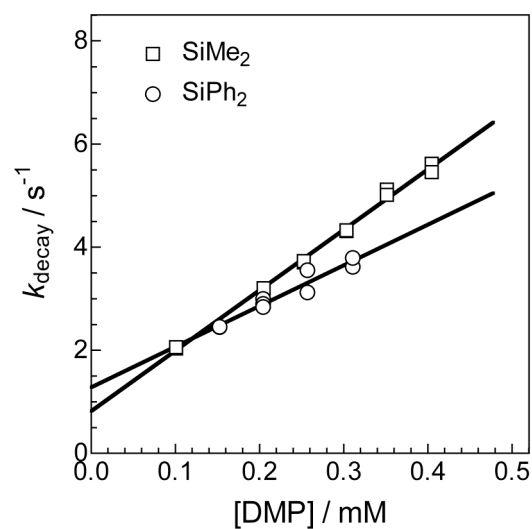
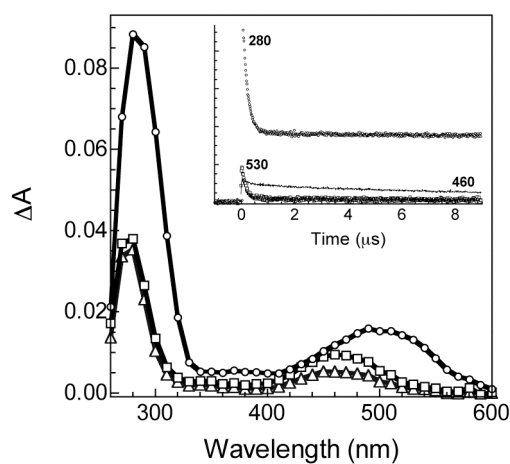
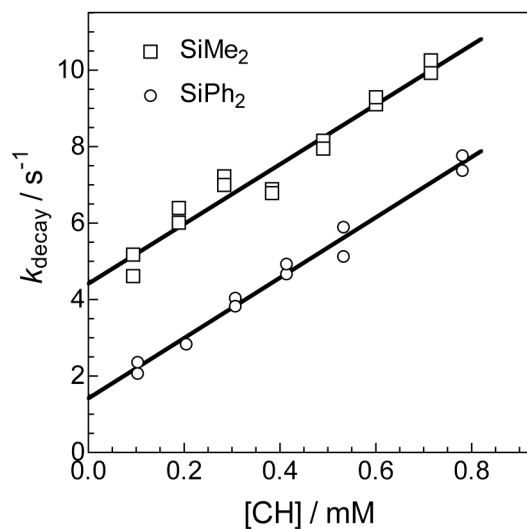


**Figure S20.** Plots of the pseudo-first order decay rate constants ( $k_{\text{decay}}$ ) for  $\text{SiMe}_2$  ( $\square$ ) and  $\text{SiPh}_2$  ( $\circ$ ) vs.  $[\text{cyclohexene}]$  in hexane solution at 25 °C. The solid lines are the linear least squares fits of the data to equation 6 in the paper.

**Figure S20.** (b) Transient absorption spectra recorded 48-112 ns ( $\circ$ ), 0.64-0.70  $\mu\text{s}$  ( $\square$ ), and 8.56-8.62  $\mu\text{s}$  ( $\Delta$ ) after the laser pulse, for a 0.09 mM solution of **9** in deoxygenated hexane containing 0.6 mM cyclohexene. The insets show decay traces recorded at 280, 530, and 460 nm.

**Figure S21.** Plot of the pseudo-first order decay rate constants ( $k_{\text{decay}}$ ) for  $\text{SiMe}_2$  ( $\square$ ) and  $\text{SiPh}_2$  ( $\circ$ ) vs.  $[\text{DMP}]$  in hexane solution at 25 °C. The solid lines are the linear least squares fits of the data to equation 6 in the paper.

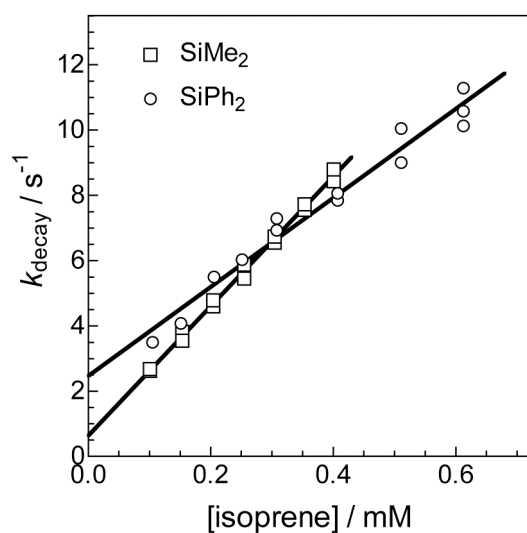
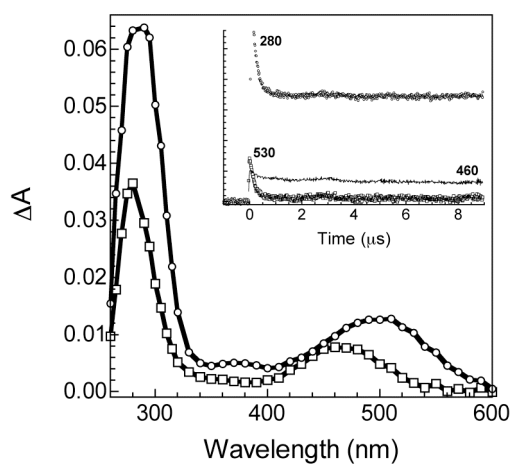
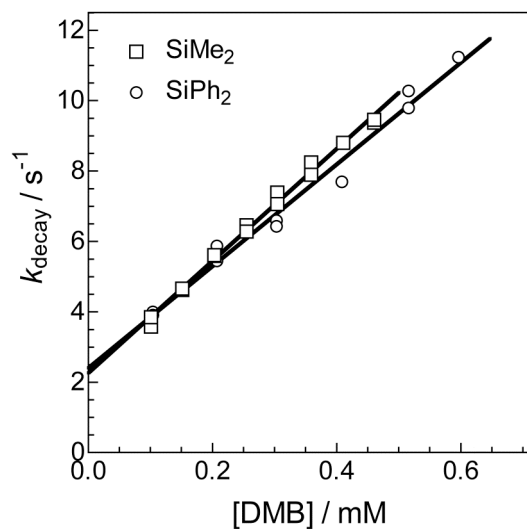


**Figure S22.** (a) Plots of the pseudo-first order decay rate constants ( $k_{\text{decay}}$ ) for SiMe<sub>2</sub> ( $\square$ ) and SiPh<sub>2</sub> ( $\circ$ ) vs. [DMB] in hexane solution at 25 °C. The solid lines are the linear least squares fits of the data to equation 6 in the paper.

**Figure S22.** (b) Transient absorption spectra recorded 64-96 ns ( $\circ$ ) and 0.62-0.74  $\mu\text{s}$  ( $\square$ ) after the laser pulse, for a 0.09 mM solution of **9** in deoxygenated hexane containing 0.4 mM DMB. The insets show decay traces recorded at 280, 530 and 460 nm.

**Figure S23.** Plots of the pseudo-first order decay rate constants ( $k_{\text{decay}}$ ) for SiMe<sub>2</sub> ( $\square$ ) and SiPh<sub>2</sub> ( $\circ$ ) vs. [isoprene] in hexane solution at 25 °C. The solid line is the linear least squares fit of the data to equation 6 in the paper.

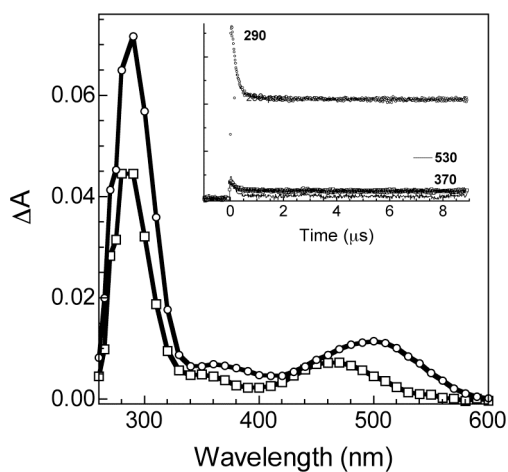
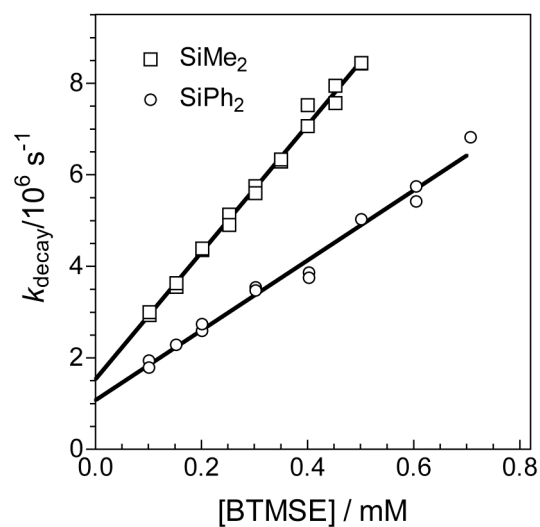


**Figure S24.** (a) Plots of the pseudo-first order decay rate constants ( $k_{\text{decay}}$ ) for  $\text{SiMe}_2$  ( $\square$ ) and  $\text{SiPh}_2$  ( $\circ$ ) vs.  $[\text{BTMSE}]$  in hexane solution at 25 °C. The solid lines are the linear least squares fits of the data to equation 6 in the paper.

**Figure S24.** (b) Transient absorption spectra recorded 16-80 ns ( $\circ$ ) and 0.51-0.62  $\mu\text{s}$  ( $\square$ ) after the laser pulse, for a 0.09 mM solution of **9** in deoxygenated hexane containing 0.8 mM BTMSE. The insets show decay traces recorded at 290, 370, and 530 nm.

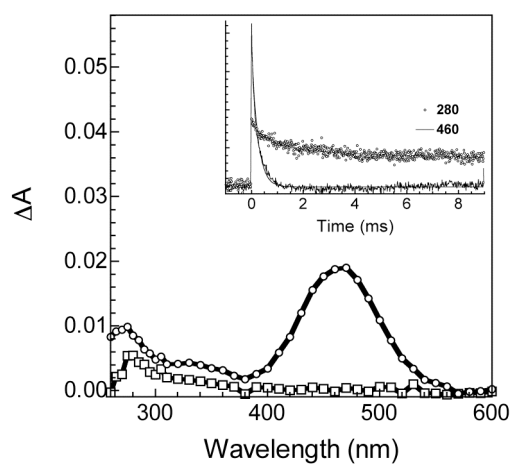
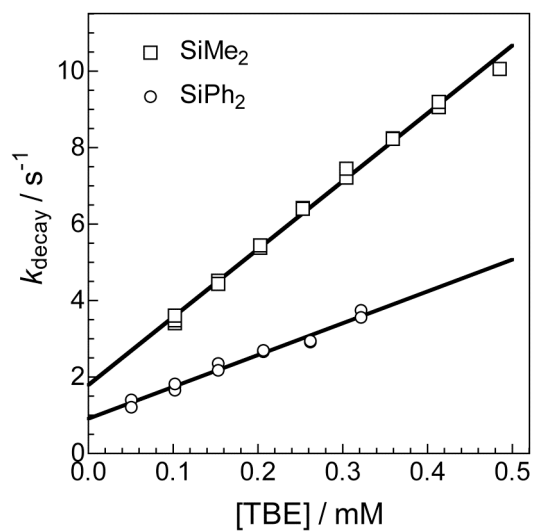


**Figure S25.** (a) Plots of the pseudo-first order decay rate constants ( $k_{\text{decay}}$ ) for SiMe<sub>2</sub> ( $\square$ ) vs. [TBE] in hexane solution at 25 °C. The solid line is the linear least squares fit of the data to equation 6 in the paper.

**Figure S25.** (b) Transient absorption spectra recorded 0-32  $\mu\text{s}$  ( $\circ$ ) and 1.01-1.12 ms ( $\square$ ) after the laser pulse, for a 0.09 mM solution of **9** in deoxygenated hexane containing 1.0 mM TBE. The insets show decay traces recorded at 280 and 480 nm.

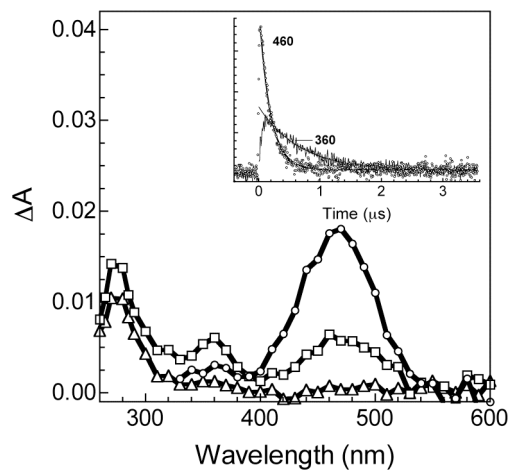


**Figure S26.** Transient absorption spectra recorded 13-26 ns ( $\circ$ ), 0.20-0.25  $\mu$ s ( $\square$ ), and 1.48-1.53  $\mu$ s ( $\Delta$ ) after the laser pulse, for a  $5 \times 10^{-4}$  M solution of **1** in deoxygenated hexane containing 0.6 mM  $\text{CCl}_4$ . The insets show decay traces recorded at 460 and 360 nm.

## References

- (1) Tamao, K.; Kawachi, A. *Organometallics* **1995**, *14*, 3108-3111.
- (2) Zhang, C.; Grumbine, S. D.; Tilley, T. D. *Polyhedron* **1991**, *10*, 1173-1176.
- (3) Zhang, S.; Conlin, R. T. *J. Am. Chem. Soc.* **1991**, *113*, 4272-4278.
- (4) Leigh, W. J.; Huck, L. A.; Held, E.; Harrington, C. R. *Silicon Chem.* **2005**, *3*, 139-149.